

# TEXTOC: Text-driven Object-Centric Style Transfer

Jihun Park\*, Jongmin Gim\*, Kyoungmin Lee\*, Seunghun Lee, Sunghoon Im†  
DGIST, Daegu, Republic of Korea

{pjh2857, jongmin4422, kyoungmin, lsh5688, sunghoonim}@dgist.ac.kr



Figure 1. Our Object-Centric style transfer results with various image-text scenarios.

## Abstract

We present *Text-driven Object-Centric Style Transfer (TEXTOC)*, a novel method that guides style transfer at an object-centric level using textual inputs. The core of TEXTOC is our *Patch-wise Co-Directional (PCD) loss*, meticulously designed for precise object-centric transformations that are closely aligned with the input text. This loss combines a patch directional loss for text-guided style direction and a patch distribution consistency loss for even CLIP embedding distribution across object regions. Key to our method are the *Text-Matched Patch Selection (TMPS)* and *Pre-fixed Region Selection (PRS)* modules for identifying object locations via text, eliminating the need for segmentation masks. Lastly, we introduce an *Adaptive*

*Background Preservation (ABP) loss* to maintain the original style and structural essence of the image’s background. This loss is applied to dynamically identified background areas. Extensive experiments underline the effectiveness of our approach in creating visually coherent and textually aligned style transfers.

## 1. Introduction

In the realm of creative digital industries such as advertising, film, and video game development, the demand for advanced image manipulation is surging. The introduction of object-focused style transfer, driven by textual commands, is transforming these sectors. It allows for detailed and user-friendly adjustments to the visual aspects of objects in images. This innovation empowers designers to bypass traditional manual editing, enabling them to define stylistic alterations using just text, thus facilitating rapid concept development and customization. Consider the

\* Equal Contribution

†Corresponding author

ease with which digital fashion elements can be modified, car hues altered for online showrooms, or furniture designs changed in virtual environments, all through simple text instructions, as illustrated in Fig. 1.

Seminal works in style transfer [6, 12, 17, 26, 33, 50, 51] have traditionally relied on reference images to guide the transfer process. While these methods have been foundational, their dependency on visual templates can constrain the creative possibilities. In contrast, a burgeoning wave of research in text-guided style transfer [3, 15, 25, 27, 32, 56] is redefining the landscape. By dispensing with the need for reference images, these novel approaches broaden the horizons for stylistic adaptations, harnessing the power of textual descriptions to steer the creative process. The pioneering approach [3] empowers object-centric editing directly steered by textual descriptions. Yet, this method also presents certain drawbacks; it risks altering the original content’s fidelity, thereby straying from the essential goal of style transfer, which is to enhance without obscuring.

To address this issue, we introduce Text-driven Object-Centric Style Transfer (TEXTOC), a novel approach aimed at transforming the appearance of objects based on textual descriptions. This approach is designed to retain the structural integrity of objects and preserve both the appearance and structure of the background. At the core of TEXTOC lie three pivotal components: the Patch-wise Co-Directional (PCD) loss, the Adaptive Background Preservation (ABP) loss, and the Text-Matched Patch Selection (TMPS) with Pre-fixed Region Selection (PRS) module.

The TMPS and PRS modules are designed to identify and style the locations of objects related to the text. Unlike traditional directional loss [16, 32] that may cause distortion due to a focus on vector directions, our PCD loss, augmented by the TMPS module, directs style transfer in foreground regions aligned with the source text. This ensures a consistent CLIP-embedding distribution across patches from both source and stylized images, promoting a cohesive style transfer within object areas. Our ABP loss is designed to preserve the style and structure of the background in the source image, specifically in non-object areas. It adaptively targets and applies the loss to dynamically detected background regions, ensuring a natural and seamless transition in object-centric style transfer and blending stylized elements with their surroundings as shown in Fig. 1.

In summary, our primary contributions include:

- We present the Text-Matched Patch Selection (TMPS) and Pre-fixed Region Selection (PRS), which identify regions of objects related to text for object-centric style transfer.
- We propose the Patch-wise Co-Directional (PCD) loss to enable precise style transfer on targeted objects, maintaining the integrity and coherence of the source’s

visual aesthetic.

- We introduce the Adaptive Background Preservation (ABP) loss, effectively maintaining the original style and structure of designated background areas.

## 2. Related Works

### 2.1. Style Transfer

Neural Style Transfer (NST) represents a significant advancement in the domain of image stylization, introduced by [17]. This pioneering approach utilized a pre-trained Convolutional Neural Network (CNN), particularly VGGNet to extract distinct content and style features. However, a notable constraint of NST lies in its substantial computational demand, stemming from the per-image optimization approach. To overcome this, [21] introduce Adaptive Instance Normalization (AdaIN), a technique that aligns the mean and variance of source image features with that of the style image. Building on this, [34, 35] propose Whitening and Coloring Transform, which aligns the entire covariance matrix of the features. This approach results in more refined and superior stylization outcomes. Another significant development is the Unbiased Image Style Transfer [1] that enhances the generalization abilities in style transfer, making it a versatile tool for various style transfer applications.

### 2.2. Text-Guided Image Synthesis

The Contrastive Language-Image Pretraining (CLIP) model, trained on a large-scale image-text dataset [42], has significantly impacted image synthesis applications [8, 14, 18, 41, 48]. Research [16, 40] building upon the StyleGAN architecture [28, 29] has shown how text descriptors can adapt the style of source images. For instance, the directional loss introduced in [16] showcases remarkable stability and diversity in this domain, overcoming the previous requirement of a style image for transfer. Parallel to these developments, the field has seen a surge in research focusing on diffusion model [19].

Recent works [4, 38, 46, 47, 53] are exploring new frontiers in image editing and generation, using text-driven diffusion models. Despite these advancements, a persisting challenge for both Generative Adversarial Networks (GANs) and diffusion models is maintaining the subject’s identity consistently in the generated images.

### 2.3. Object-Centric Style Transfer

Recent advancements in object-centric style transfer have seen a surge in customizable techniques. Initial methods [23, 24, 31] rely on reference images for style information, applying style transfer to targeted areas through segmentation networks or additional clustering methods. StyleGAN-NADA [16] marks a paradigm shift in this ap-

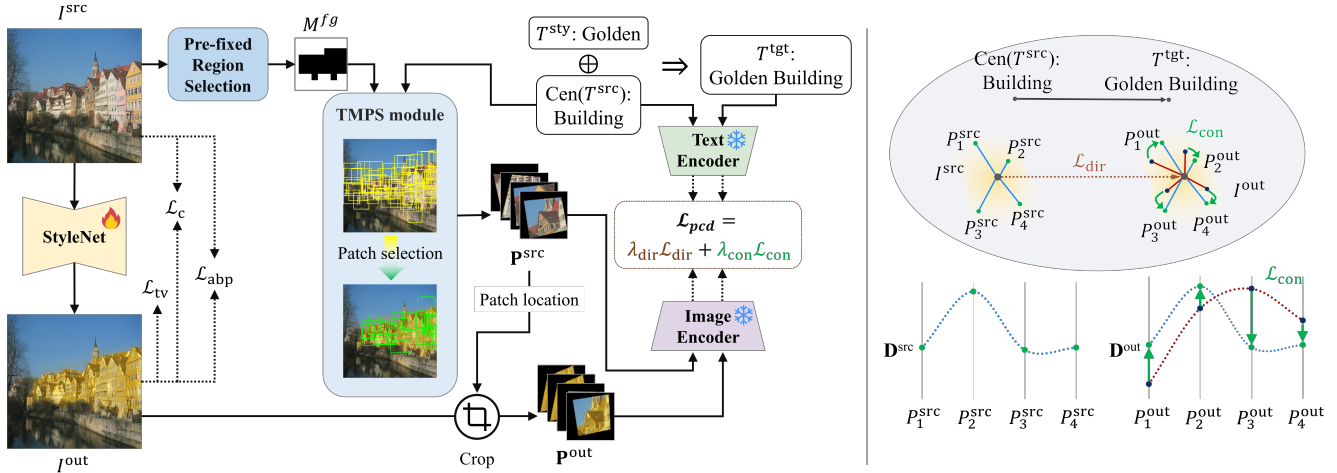


Figure 2. **(Left)** Overall pipeline of our TEXTOC consisting of a stylization network (StyleNet), Pre-fixed Region Selection (PRS), Text-Matched Region Selection (TMPS) module and pretrained CLIP encoders. The StyleNet takes a source image  $I^{\text{src}}$  and generates an object-wise stylized image  $I^{\text{out}}$ . The TMPS module is responsible for pinpointing patches that most closely correspond to  $T^{\text{src}}$  from the foreground regions identified by the PRS. The selected and augmented patches,  $\mathbf{P}^{\text{src}}, \mathbf{P}^{\text{out}}$ , are then aligned with  $T^{\text{src}}, T^{\text{tgt}}$  in the CLIP embedding space using Patch-wise Co-Directional (PCD) loss  $\mathcal{L}_{\text{pcd}}$ . The target text  $T^{\text{tgt}}$  is derived by central word selection. Additionally, we apply a content loss  $\mathcal{L}_c$ , an Adaptive Background Preservation (ABP) loss  $\mathcal{L}_{\text{abp}}$  to enhance object-wise style transfer, along with a total variance loss  $\mathcal{L}_{\text{tv}}$  for regularization. **(Right)** Illustration of the functionality of the PCD loss in feature space. It is composed of a patch-wise directional loss  $\mathcal{L}_{\text{dir}}$  and a patch distribution consistency loss  $\mathcal{L}_{\text{con}}$ .

proach by eliminating the need for reference images and instead utilizing textual directions in the CLIP space for style transfer. This is further advanced by CLIPstyler [32] which successfully applied this novel concept in the style transfer domain. Following this trajectory, the works [27, 54] have introduced style transfer with segmentation map but without the dependency on reference images. A unique approach [3] extracts a relevancy map [5] based on the input text. It allows for stylization focused only on the text-corresponding object regions, moving away from traditional segmentation methods. However, a notable limitation of these techniques is the unintended alteration of both the style and the content information of the object.

### 3. Method

#### 3.1. Overview Framework

The overall pipeline of our model is illustrated in Fig. 2- (Left). We train a stylization network (StyleNet) to generate a stylized image  $I^{\text{out}}$ , given a source image  $I^{\text{src}}$ , along with accompanying source text  $T^{\text{src}}$ , and a style text  $T^{\text{sty}}$ . We use the text encoder and the image encoder derived from the pre-trained CLIP model, freezing their parameters during the training process. The training of StyleNet incorporates a composite loss function consisting of four distinct components: Patch-wise Co-Directional loss ( $\mathcal{L}_{\text{pcd}}$ ), Adaptive Background Preservation loss ( $\mathcal{L}_{\text{abp}}$ ), a content loss ( $\mathcal{L}_c$ ), and a total variation regularization loss ( $\mathcal{L}_{\text{tv}}$ ). These are

weighted by the balance terms  $\lambda_{\text{abp}}, \lambda_c$  and  $\lambda_{\text{tv}}$  as follows:

$$\mathcal{L}_{\text{total}} = \mathcal{L}_{\text{pcd}} + \lambda_{\text{abp}}\mathcal{L}_{\text{abp}} + \lambda_c\mathcal{L}_c + \lambda_{\text{tv}}\mathcal{L}_{\text{tv}}. \quad (1)$$

This paper primarily delves into the Patch-wise Co-Directional loss  $\mathcal{L}_{\text{pcd}}$  in Sec. 3.3, and the Adaptive Background Preservation loss  $\mathcal{L}_{\text{abp}}$  in Sec. 3.4. The content loss  $\mathcal{L}_c$  imposes the mean-square error between the features of an input and a stylized image extracted from the pre-trained VGG-19 networks [17]. The total variation loss  $\mathcal{L}_{\text{tv}}$  is a loss function designed based on the noise removal method [45].

#### 3.2. Text-Matched Region Selection (TMPS)

A critical aspect of object-centric style transfer is the accurate identification of the object’s location within an image. To address this challenge, we introduce the TMPS module, which is engineered to pinpoint and select image patches correlating to a specified object as described by the source text. Utilizing the image encoder  $E_I$  and the text encoder  $E_T$  from the CLIP architecture, TMPS establishes a strong link between the object and its textual descriptor. We define a representative feature vector  $f_{\text{avg}}$  in Alg. 1, capturing the essential characteristics of the object in the source image. Then, we identify patches  $\mathbf{P}^{\text{sel}}$  with features similar to this representative vector. The detailed mechanism of TMPS is explained in Alg. 1.

To streamline the search process for TMPS during the object-centric style transfer, we introduce the Pre-fixed Region Selection (PRS) module within the source image. Ap-

---

**ALGORITHM 1: Text-Matched Patch Selection**

---

**Input:** Image patch set  $\mathbf{P}$  and source text  $T^{\text{src}}$   
**Output:** Patches corresponding to the source text  $\mathbf{P}^{\text{sel}}$   
**Parameter:**  $K$ : # of patches in  $\mathbf{P}$ ,  
 $M$ : # of patches similar to source text

- 1:  $\mathbf{S}, \hat{\mathbf{S}} \leftarrow \emptyset, \emptyset$
- 2: **for**  $i = 1$  to  $K$  **do**
- 3:  $f_i \leftarrow E_I(P_i)$
- 4:  $s_i \leftarrow \frac{f_i \cdot E_T(T^{\text{src}})}{\|f_i\| \cdot \|E_T(T^{\text{src}})\|}$
- 5:  $\mathbf{S} \leftarrow \mathbf{S} \cup \{s_i\}$
- 6: **end for**
- 7:  $\mathbf{I} \leftarrow \{i \mid s_i \geq \text{the } M^{\text{th}} \text{ largest value in } \mathbf{S}\}$
- 8:  $f_{\text{avg}} \leftarrow \frac{1}{|\mathbf{I}|} \sum_{i \in \mathbf{I}} f_i$
- 9: **for**  $j = 1$  to  $K$  **do**
- 10:  $\hat{s}_j \leftarrow \frac{f_j \cdot f_{\text{avg}}}{\|f_j\| \cdot \|f_{\text{avg}}\|}$
- 11:  $\hat{\mathbf{S}} \leftarrow \hat{\mathbf{S}} \cup \{\hat{s}_j\}$
- 12: **end for**
- 13:  $\hat{s}_k \leftarrow \text{the } (\text{round}(\frac{K}{2}))^{\text{th}} \text{ largest value from } \hat{\mathbf{S}}$
- 14:  $\mathbf{J} \leftarrow \{j \mid \hat{s}_j \geq \hat{s}_k \text{ and } \hat{s}_j > 0.8\}$
- 15: **return**  $\mathbf{P}^{\text{sel}} \leftarrow \{P_j \mid j \in \mathbf{J}\}$

---

plied mainly during the initial iterations, this module delineates a foreground region  $M^{\text{fg}}$ , configured to coarsely isolate object areas as outlined in Alg. 2. This early demarcation of the object’s location allows for generating patches specifically within the foreground region ( $M^{\text{fg}}$ ) in later iterations. This strategy enhances the precision and efficiency of the style transfer, focusing the modification on the most relevant sections of the image.

### 3.3. Patch-Wise Co-Directional Loss (PCD)

Our PCD loss  $\mathcal{L}_{\text{pcd}}$  incorporates a patch-wise directional loss  $\mathcal{L}_{\text{dir}}$  and a patch distribution consistency loss  $\mathcal{L}_{\text{con}}$  with balance terms  $\lambda_{\text{dir}}$  and  $\lambda_{\text{con}}$  as follows:

$$\mathcal{L}_{\text{pcd}} = \lambda_{\text{dir}} \mathcal{L}_{\text{dir}} + \lambda_{\text{con}} \mathcal{L}_{\text{con}}. \quad (2)$$

**Patch-wise directional loss** The foundational concept of directional loss, as initially introduced in [16] and [32], is further refined in our approach. We adapt and advance this concept specifically for object-centric style transfer, with a targeted application on image patches that correspond to the source text  $T^{\text{src}}$ . We commence by randomly selecting a subset of patches within the foreground region  $M^{\text{fg}}$  of the source image. The selected patches, represented as  $\mathbf{P}^{\text{src}} \in \{P_1^{\text{src}}, \dots, P_N^{\text{src}}\}$ , are then extracted using our TMPS, as detailed in Alg. 1. Given the patches and the texts, the

---

**ALGORITHM 2: Pre-fixed Region Selection**

---

**Input:** Source image  $I^{\text{src}}$  and source text  $T^{\text{src}}$   
**Output:** A binary mask containing objects corresponding to the source text  $M^{\text{fg}}$   
**Parameter:**  $\tau$ : Threshold for # of selections.

- 1: Divide  $I^{\text{src}}$  into  $L$  uniform square grids.
- 2: Generate a set of three distinct-sized patches per grid:  $\mathbf{P}^{\text{grid}} = \{P_1^{\text{grid}}, \dots, P_{3L}^{\text{grid}}\}$ .
- 3: Obtain selected patches  $\mathbf{P}^{\text{grid.sel}}$  using TMPS module:  $\mathbf{P}^{\text{grid.sel}} = \text{TMPS}(\mathbf{P}^{\text{grid}}, T^{\text{src}})$ .
- 4: Initialize a voting matrix  $V \in \mathbb{R}^{H \times W}$  with all elements set to zero.
- 5: **for** each pixel in the selected patches  $\mathbf{P}^{\text{grid.sel}}$  **do**
- 6: Increment the corresponding element in  $V$ .
- 7: **end for**
- 8: Determine the pre-fixed foreground region  $M^{\text{fg}}$ :

$$M^{\text{fg}}(i, j) = \begin{cases} 1, & \text{if } V(i, j) \geq \tau \\ 0, & \text{otherwise} \end{cases}$$

- 9: **return**  $M^{\text{fg}}$

---

patch-wise directional loss  $\mathcal{L}_{\text{dir}}$  is defined as follows:

$$\mathcal{L}_{\text{dir}} = \frac{1}{N} \sum_{i=1}^N \left( 1 - \frac{\Delta P_i \cdot \Delta T}{|\Delta P_i| |\Delta T|} \right),$$

$$\Delta P_i = E_I(\text{aug}(P_i^{\text{out}})) - E_I(\text{aug}(P_i^{\text{src}})),$$

$$\Delta T = E_T(T^{\text{tgt}}) - E_T(T^{\text{src}}), \quad T^{\text{tgt}} = T^{\text{sty}} \oplus \text{Cen}(T^{\text{src}}), \quad (3)$$

where the operator  $\oplus$  denotes text combination. We utilize the function  $\text{Cen}(\cdot)$  for central word selection and  $\text{aug}(\cdot)$  for patch augmentation. The patches  $P_i^{\text{out}}$  are derived from output stylized images  $I^{\text{out}}$  using the TMPS algorithm in Alg. 1.

**Target text generation** To formulate the target text  $T^{\text{tgt}}$ , we apply central word selection technique  $\text{Cen}(\cdot)$  in (3) leveraging Spacy [20], and merge the source text  $T^{\text{src}}$  and the style text  $T^{\text{sty}}$ . This design is rooted in the manifold augmentation technique proposed in [55] leveraging text embeddings from models like BERT [9], GPT [43], and CLIP. This amalgamation of texts aligns more closely with the user’s intended styling objectives. For instance, to adapt the style of ‘red apple’ to appear green, we engage TMPS using ‘red apple’ but modify the target text to ‘green apple’, with an emphasis on ‘apple’ as the central word. This refined approach to text input in TMPS enables more accurate patch selection, facilitating precise object-centric style transfer.

**Patch distribution consistency loss** Traditional directional loss functions typically emphasize the direction of vectors while often neglecting their semantic information. This em-

phases can inadvertently lead to a misalignment between patches in the source image and those in the stylized image as depicted in Fig. 2-(Right). Such a discrepancy can lead to the collapse of semantic information, resulting in a distorted transformation that causes the loss of information from the source image, contradicting the fundamental aim of style transfer. To address this issue, we design the patch distribution consistency loss  $\mathcal{L}_{\text{con}}$  as follows:

$$\begin{aligned} \mathcal{L}_{\text{con}} &= \text{JSD}(\mathbf{D}^{\text{src}}, \mathbf{D}^{\text{out}}), \\ \mathbf{D}^{\text{src}} &= \frac{\hat{\mathbf{D}}^{\text{src}}}{\sum_{i=1}^N \hat{\mathbf{D}}_i^{\text{src}}}, \hat{\mathbf{D}}^{\text{src}} = \left( \frac{E_I(P_i^{\text{src}}) \cdot E_I(I^{\text{src}})}{|E_I(P_i^{\text{src}})| \cdot |E_I(I^{\text{src}})|} \right)_{i=1}^N, \\ \mathbf{D}^{\text{out}} &= \frac{\hat{\mathbf{D}}^{\text{out}}}{\sum_{i=1}^N \hat{\mathbf{D}}_i^{\text{out}}}, \hat{\mathbf{D}}^{\text{out}} = \left( \frac{E_I(P_i^{\text{out}}) \cdot E_I(I^{\text{out}})}{|E_I(P_i^{\text{out}})| \cdot |E_I(I^{\text{out}})|} \right)_{i=1}^N, \end{aligned} \quad (4)$$

where  $\text{JSD}(\cdot)$  is Jensen–Shannon divergence, which is employed to align the feature distributions of patches  $\mathbf{D}^{\text{src}}$  from the source image with those  $\mathbf{D}^{\text{out}}$  from the stylized image.

### 3.4. Adaptive Background Preservation (ABP) Loss

We introduce the ABP loss, designed to ensure the non-stylization of the background region. Our approach begins by identifying a pre-fixed foreground  $M^{\text{fg}}$ , as outlined in Alg. 2. In each iteration, the adaptive foreground mask  $M^{\text{fg}*}$  and background mask  $M^{\text{bg}*}$  are dynamically updated as follows:

$$M^{\text{bg}*} = 1 - M^{\text{fg}*}, M^{\text{fg}*} = \left( \bigvee_{i=1}^{N_{\text{iter}}} M_i^{\text{src}} \right), \quad (5)$$

where  $N_{\text{iter}}$  represents the number of patches in each iteration, and the binary mask  $M_i^{\text{src}}$  is assigned a value of one over the area of patches  $\{P_i^{\text{src}}\}_{i=1, \dots, N_{\text{iter}}}$ , which are selected from the source image through the TMPS.

Next, we apply the MS-SSIM and L1 loss functions to ensure that the original styles of background regions are retained as follows:

$$\begin{aligned} \mathcal{L}_{\text{abp}} &= \mathcal{L}_{\text{MS-SSIM}}(I^{\text{out}} \odot M^{\text{bg}*}, I^{\text{src}} \odot M^{\text{bg}*}) \\ &+ \mathcal{L}_{\text{L1}}(I^{\text{out}} \odot M^{\text{bg}*}, I^{\text{src}} \odot M^{\text{bg}*}). \end{aligned} \quad (6)$$

This loss enables a well-balanced integration of the stylized and original regions within the image. Specifically, while the foreground areas undergo stylization, the background’s integrity is preserved.

## 4. Experiments

### 4.1. Implementation Details

We employ the pretrained CLIP model on ViT-B/32 [11]. Our stylization network is based on the U-net architecture [44] consisting of three downsample and three

upsample layers featuring channel sizes of 16, 32, and 64. The source images have a resolution of  $512 \times 512$  pixels. We set  $\lambda_{\text{dir}}$ ,  $\lambda_{\text{con}}$ ,  $\lambda_{\text{abp}}$ ,  $\lambda_{\text{c}}$ , and  $\lambda_{\text{tv}}$  to  $1.5 \times 10^4$ ,  $3 \times 10^4$ ,  $3 \times 10^4$ ,  $4 \times 10^2$ , and  $2 \times 10^{-3}$ , respectively. For content loss, we follow [17] by utilizing features from the “conv4\_2” and “conv5\_2” layers.

We commence our training with an initial set of 20 early iterations and completed a total of 200 iterations using the Adam optimizer [30]. The training began with an initial learning rate of  $5 \times 10^{-4}$ , halved after the first 100 iterations. We incorporate the perspective augmentation function from the PyTorch library [39]. Notably, our model treats each scene independently, processing them on a per-scene basis. On average, the training time for each text prompt is approximately 45 seconds when conducted on an NVIDIA A6000 GPU. For further details on our training procedure, please refer to the supplementary material.

### 4.2. Evaluation metrics

We conduct a comprehensive quantitative evaluation using a variety of metrics that are well-established in the field of text-driven style transfer as outlined in Tab. 1. The similarity metric (Sim) quantifies the likeness between the image and text embedding vectors, assessing the congruence of the two embeddings. We also apply content metrics (Con) using the VGG content loss [26] and style metrics (Sty) using the mean-variance style loss [22]. These metrics are adapted from traditional calculations but specifically mask either the foreground or background of input images to focus analysis on selected areas. To thoroughly evaluate the quality of the stylized image backgrounds from multiple aspects, we conduct additional assessments specifically targeting the background masks. For this purpose, we utilize the SSIM metric [52], which evaluates structural, luminance, and color attributes. Additionally, we employ the DISTS measure [10] to ensure deep structural and textural consistency in these areas. Furthermore, we use the PSNR [13] metric and absolute difference (L1) for an overall assessment of signal fidelity and basic visual quality in the backgrounds.

For a comprehensive quantitative evaluation of object-centric style transfer, we split the image region into foreground and background components. We utilize Ground Truth (GT) segmentation (binary) masks for the object  $M^{\text{fg-gt}}$  and background  $M^{\text{bg-gt}} (= 1 - M^{\text{fg-gt}})$ . For example, the  $\text{SIM}_F$  and  $\text{L1}_B$  are formulated as follows:

$$\begin{aligned} \text{Sim}_F &= \frac{E_T(T_i^{\text{tgt}}) \cdot E_I(I^{\text{out}} \odot M^{\text{fg-gt}})}{|E_T(T_i^{\text{tgt}})| \cdot |E_I(I^{\text{out.f}})|}, \\ \text{L1}_B &= \frac{\sum |I^{\text{src}} \odot M^{\text{bg-gt}} - I^{\text{out}} \odot M^{\text{bg-gt}}|}{255 \cdot \text{num}(I^{\text{src}} \odot M^{\text{bg-gt}})}, \end{aligned} \quad (7)$$

where  $E_I$  and  $E_T$  denote the pre-trained CLIP image and text encoders, respectively.  $\text{num}(\cdot)$  indicates the number

Methods	Foreground quality metrics		Background quality metrics					
	Sim <sub>F</sub> ↑	Con <sub>F</sub> ↓	L1 <sub>B</sub> ↓	Con <sub>B</sub> ↓	Sty <sub>B</sub> ↓	SSIM <sub>B</sub> ↑	DISTS <sub>B</sub> ↓	PSNR <sub>B</sub> ↑
FlexIT [7]	0.24	8.08	0.25	4.78	0.73	0.60	0.17	19.69
Null-text inversion [37]	0.20	4.22	0.16	2.58	0.22	0.74	0.10	23.48
Instruct Pix2Pix [4]	0.22	7.42	0.44	4.66	0.97	0.62	0.20	17.25
Plug and Play [49]	0.23	6.51	0.33	4.26	0.63	0.63	0.22	18.26
ZeCon [53]	0.23	7.49	0.28	5.33	0.63	0.64	0.24	19.35
CLIPstyler [32]	0.28	5.16	0.66	3.27	0.35	0.51	0.25	13.20
Text2live [3]	<u>0.32</u>	<u>4.13</u>	<u>0.14</u>	<u>1.22</u>	<u>0.18</u>	<u>0.87</u>	<u>0.09</u>	<u>24.69</u>
Ours	<b>0.33</b>	<b>3.75</b>	<u>0.10</u>	<u>1.15</u>	<u>0.10</u>	<u>0.90</u>	<u>0.07</u>	<u>27.65</u>

Table 1. Quantitative comparison of our method with the recent text-guided style transfer methods using foreground quality metrics and background quality metrics. The symbols ↑ and ↓ indicate higher values are better and lower values are better, respectively.



Figure 3. Comparison of our method with various text-guided style transfer models. To the left of the solid line are the qualitative results of our model and non-diffusion based models, to the right are the results from diffusion-based methods.

of pixels in the image. We randomly selected 16 images from the MSCOCO 2017 dataset [36], each accompanied by GT segmentation masks, to conduct evaluation. Each image was paired with a total of 10 style text descriptions based on three different categories: color (red, blue, green), texture (golden, frosted, stained glass, neon light), and artistic style (Starry Night by Vincent van Gogh, a watercolor painting of flowers, cubism style). This resulted in a total of 160 stylized images for evaluation.

### 4.3. Comparison to state-of-the-arts

In Tab. 1 and Fig. 3, we present both quantitative and qualitative comparisons of our TEXTOC model against various text-driven stylization models including various diffusion models, such as Text2LIVE [3], CLIPstyler [32], ZeCon [53], Plug and Play [49], Instruct Pix2Pix [4], Null-text

inversion [37] and FlexIT [7]. Our quantitative evaluation indicates that our method surpasses all compared models in performance. Specifically, the object regions in stylized images from our method exhibit higher Sim<sub>F</sub> and lower Con<sub>F</sub> scores compared to competitive methods. This indicates that our proposed method effectively styles the object regions according to the corresponding text while preserving the structure of the source image. In terms of background quality, the metrics show that the proposed method subtly changes the style of background regions in the source image, as indicated by Sty<sub>B</sub>. Meanwhile, it maintains the integrity of the source image’s structure, as evidenced by scores from L1<sub>B</sub>, Con<sub>B</sub>, SSIM<sub>B</sub>, DISTS<sub>B</sub>, and PSNR<sub>B</sub>. This dual capability highlights our method’s adeptness at enhancing foreground elements distinctly from the background, ensuring a balanced and coherent visual output.

Components #	Components			Foreground quality metrics		Background quality metrics					
	$\mathcal{L}_{dir}$	$\mathcal{L}_{con}$	$\mathcal{L}_{abp}$	Sim <sub>F</sub> ↑	Con <sub>F</sub> ↓	L1 <sub>B</sub> ↓	Con <sub>B</sub> ↓	Sty <sub>B</sub> ↓	SSIM ↑	DISTS ↓	PSNR ↑
(a)				0.29	4.31	0.60	2.72	0.25	0.56	0.22	14.16
(b)	✓			<u>0.32</u>	4.72	0.49	2.07	0.21	0.64	0.15	16.02
(c)	✓	✓		<b>0.33</b>	4.62	0.48	2.00	0.21	0.65	0.15	16.16
(d)	✓		✓	<u>0.32</u>	<u>4.16</u>	<b>0.10</b>	<u>1.28</u>	<u>0.12</u>	<u>0.89</u>	<u>0.08</u>	<u>27.28</u>
(e)	✓	✓	✓	<b>0.33</b>	<b>3.75</b>	<b>0.10</b>	<b>1.15</b>	<b>0.10</b>	<b>0.90</b>	<b>0.07</b>	<b>27.65</b>

Table 2. Ablation study examining the effects of the proposed losses  $\mathcal{L}_{dir}$ ,  $\mathcal{L}_{con}$ , and  $\mathcal{L}_{abp}$ . The quantitative results of (a)-(e) correspond to the qualitative results shown in Fig. 4. The symbols ↑ and ↓ indicate higher values are better and lower values are better, respectively.

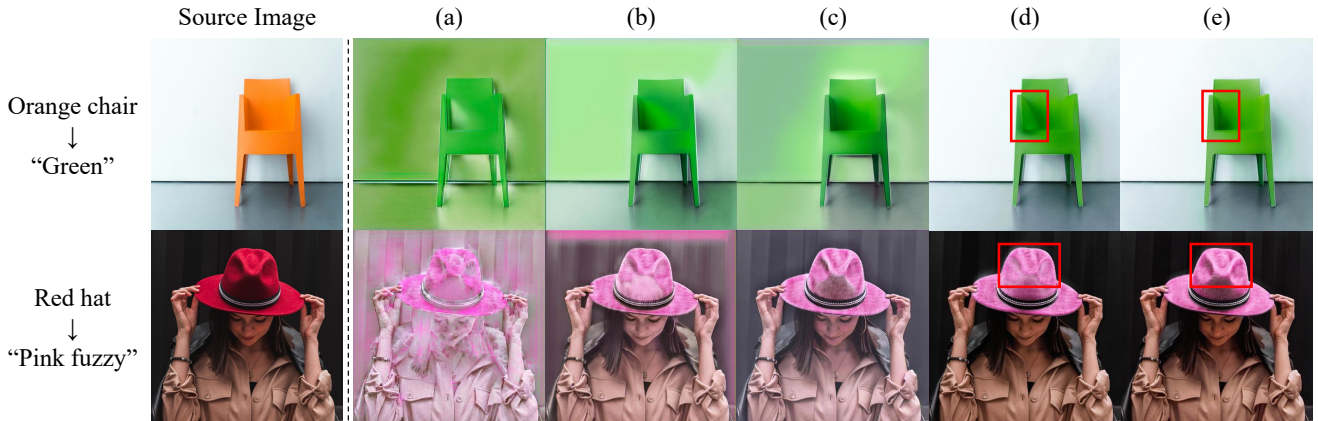


Figure 4. Qualitative results showcasing the impact of applying/omitting the proposed losses. Configurations (a)-(e) correspond to the settings detailed in Tab. 2.

In the qualitative evaluation, the first row of Fig. 3 showcases the transformation of a mountain into a volcano using the style text “Volcano”. Our method adeptly preserves the inherent structure of the mountain while seamlessly integrating the volcanic style. In contrast, Text2LIVE often reconstructs an entirely new mountain structure, typically characterized by a singular hole indicative of magma. For the five diffusion-based style transfer models, it is noticeable that the images either do not look realistic or fail to adequately reflect the style of a volcano. This comparison underscores the nuanced capability of our approach in maintaining the original form while applying distinct style transformations. Utilizing source texts like “wooden door”, “croissant” and “red umbrella”, our method demonstrates a precise capture of object locations, contrasting with other models that often indiscriminately apply style transfer to the entire image. While Text2LIVE shows results similar to ours, it notably applies style transfer to unintended areas (e.g., wooden door with “gray marble” as style text) and fail to properly reflect the style indicated by the style text (e.g., red umbrella in “Starry night by vincent Van Gogh”).

#### 4.4. Ablation study

To demonstrate the efficacy of our method, we conduct an ablation study, with quantitative results presented in Tab. 2 and qualitative insights in Fig. 4. Notably, the quantitative results in Tab. 2-(e) which incorporates all proposed losses  $\mathcal{L}_{dir}$ ,  $\mathcal{L}_{con}$ , and  $\mathcal{L}_{abp}$ , indicate that our method achieves the best performance. Notably, the absence of the adaptive background preservation loss  $\mathcal{L}_{abp}$  in Tab. 2-(c) results in a significant drop in the background similarity metric Sim<sub>B</sub>. Omitting the patch distribution consistency loss  $\mathcal{L}_{con}$  in Tab. 2-(d) leads to a decrease in performance across all foreground quality metrics. These findings clearly demonstrate the critical role of each proposed loss, affirming their essential contributions to our design.

The qualitative results in Fig. 4 further illustrate this point. In Fig. 4-(a), a scenario where patches are randomly selected and directional loss based on the text direction is applied without incorporating all proposed losses and modules, demonstrates a significant limitation. Here, the entire source image undergoes stylization, which leads to a distortion of the semantic content originally present in the image. Fig. 4-(b) demonstrates that applying only  $\mathcal{L}_{dir}$  leads to focused stylization on the targeted object, enabled by TMPS,

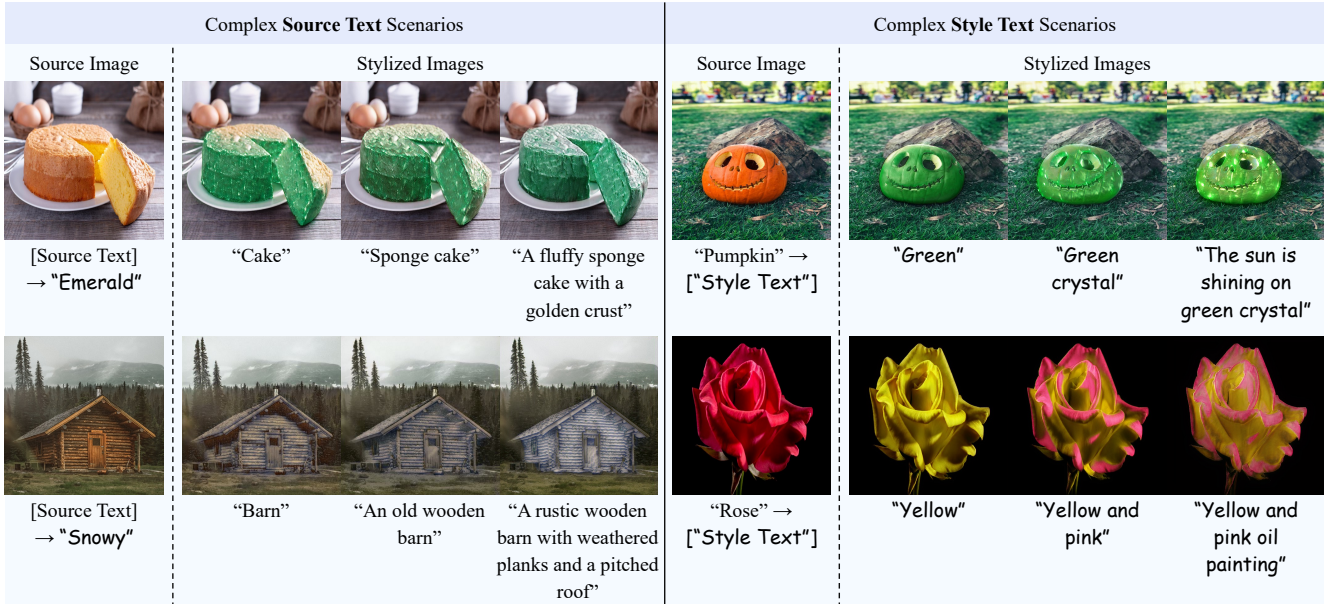


Figure 5. Our stylization results with complex image-text scenarios.

but also results in notable background changes and some loss or alteration of object details. In contrast, Fig. 4-(c), where  $\mathcal{L}_{\text{dir}}$  is combined with  $\mathcal{L}_{\text{con}}$ , effectively preserves crucial object details like the chair’s shadow and shape of the hat, though background alterations remain. The comparison of Fig. 4-(d) and (e) reveals the impact of the  $\mathcal{L}_{\text{con}}$ ; in (d), despite achieving object-centric stylization, there is a noticeable loss in object details, particularly in cropped areas. Meanwhile, the comparison of Fig. 4-(c) and (e) demonstrates that with the full complement of losses, both the background remains unchanged and the object details are preserved without distortion, highlighting the effectiveness of the ABP loss.

#### 4.5. Complex input texts

We have conducted further experiments using a diverse set of examples featuring intricate ‘source’ and ‘style’ texts results in Fig. 5. For example, in the ‘cake to emerald’ scenario, although the stylized image with simple text retains aspects of the original cake’s style, the detailed source text enables the creation of a cake styled purely in emerald. Similarly, in the ‘barn to snowy’ scenario, the model adeptly preserves the background’s style while effectively applying stylization to the foreground object. Furthermore, our experiments incorporating complex ‘style’ texts illustrate the complexity of the text does not impede our method’s ability to achieve the intended stylization effects. These results clearly demonstrate that our method is adept not only at managing simple texts but is equally effective with complex textual inputs. This expansion of our testing framework un-

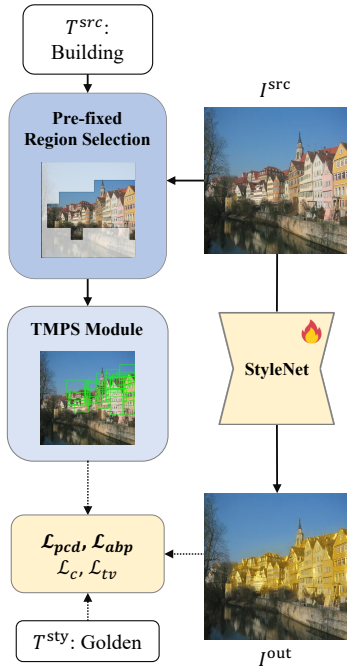
derscores our method’s robustness and versatility in accommodating a broad spectrum of textual complexities.

## 5. Conclusion

In this paper, we have presented Text-driven Object-Centric Style Transfer (TEXTOC), a new approach for transforming the appearance of objects in images based purely on textual descriptions. This method eliminates the need for reference style images or segmentation masks, facilitating complex and tailored stylizations directly from text. At the heart of TEXTOC are three pivotal components: the Text-Matched Patch Selection with Pre-fixed Region Selection module, the Patch-wise Co-Directional (PCD) loss and the Adaptive Background Preservation (ABP) loss. The TMPS and PRS modules are pivotal in accurately identifying the location of objects linked to the source text. The PCD loss, complemented by our Text-Matched Patch Selection (TMPS), precisely identifies and selects patches for stylization, ensuring an artifact-free style transfer through consistent CLIP-embedding distribution. Meanwhile, the ABP loss plays a critical role in preserving the original style and structure of the background. It adeptly adjusts to dynamically identified background areas, effectively preventing unintended alterations during the style transfer process. Extensive experiments validate the superior performance of our TEXTOC, demonstrating its capability to achieve high-quality, text-driven object-centric stylization while preserving the overall visual coherence and integrity of images.

# Supplementary Material

## A. Detailed training process of the TEXTOC



- The model takes three inputs: a source image ( $I^{src}$ ), which is the subject of the style transfer; a source text ( $T^{src}$ ), which identifies the specific object in the source image to be modified; and a style text ( $T^{sty}$ ), describing the desired style to be applied to the object.
- In the early iterations, the Pre-fixed Region Selection (PRS) is used to divide  $I^{src}$  into coarse foreground and background regions.
- Within the coarsely segmented foreground region, patches are generated. The Text-Matched Patch Selection (TMPS) module then comes into play, selecting those patches that correspond to the object mentioned in  $T^{src}$ .
- The training of the model incorporates a combination of loss functions: Patch-wise Co-Directional loss ( $\mathcal{L}_{pcd}$ ), Adaptive Background Preservation loss ( $\mathcal{L}_{abp}$ ), Content loss ( $\mathcal{L}_c$ ), and Total Variation loss ( $\mathcal{L}_{tv}$ ).

Figure 6. Simplified overview of the training process.

### A.1. Pre-fixed Region Selection (PRS)

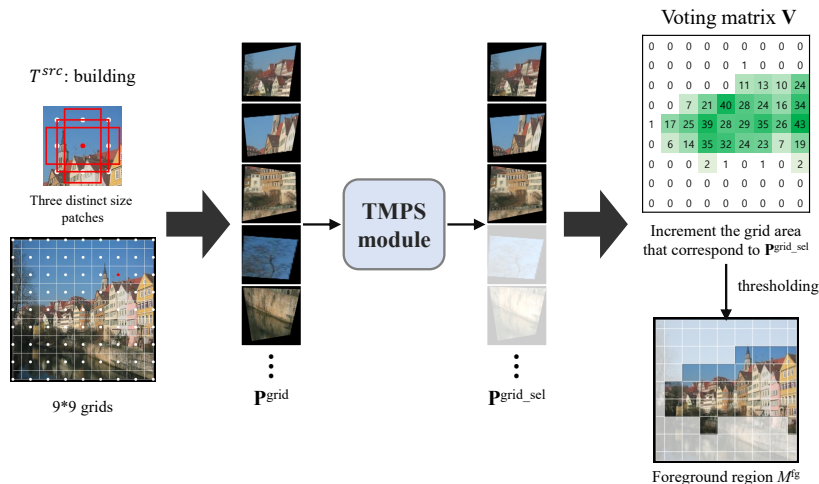


Figure 7. Overview of Pre-fixed Region Selection (PRS).

In our approach, we process the source image ( $I^{src}$ ) by dividing it into a  $9 \times 9$  grid. From each grid point, we generate three patches of varying sizes, centered on these points, resulting in a total of 243 patches. These patches are then passed

through the Text-Matched Patch Selection (TMPS) module, which identifies and selects the patches that are most relevant to the source text ( $T^{src}$ ). We use a specific threshold to determine the foreground region ( $M^{fg}$ ) of the image: grids that exceed this threshold in terms of patch relevance are classified as part of the foreground. After the initial iterations, further patch generation is concentrated within this coarse foreground region. The number of patches generated in subsequent iterations is adjusted proportionally to the count of grids identified as part of the foreground region. This method ensures a focused and relevant application of style transfer where it is most pertinent according to the text input.

## B. Comprehensive Analysis of our TEXTOC

In our study, we conduct experiments specifically designed to evaluate the impact of the patch distribution consistency loss within our TEXTOC model. The primary objective of these experiments was to ascertain how this loss function influences the overall effectiveness of the model in achieving high-quality stylization. Additionally, we present the stylization results at various stages of the model’s training process. This presentation is instrumental in demonstrating the progressive impact of the proposed loss function. Through these results, we aim to showcase how the patch distribution consistency loss enhances the model’s capability to deliver consistently high-quality stylizations. This detailed examination and presentation of results not only highlight the efficacy of the patch distribution consistency loss in our TEXTOC model but also provide valuable insights into the model’s operational dynamics throughout its training phase.

### B.1. The patch distribution consistency loss

To demonstrate the impact of the patch distribution consistency loss, denoted as  $\mathcal{L}_{con}$ , we conduct an ablation study. The findings from this study are displayed in Fig. 8. A key observation from our experiments is that the inclusion of  $\mathcal{L}_{con}$  significantly contributes to the preservation of vital features in the images, even after the style transformation process. Notable examples include the retention of text on a T-shirt, the intricate pattern of a tropical fish, and the clarity of numbers on a bowling ball. These results highlight that the implementation of the  $\mathcal{L}_{con}$  loss is crucial in maintaining a focused distribution of patches on the object. This focused approach is what enables the preservation of essential details and textures during the style transformation, ensuring that the core visual elements of the object remain intact and recognizable post-transformation. This study thus underscores the effectiveness of the  $\mathcal{L}_{con}$  loss in enhancing the quality and fidelity of object-centric style transfers in our TEXTOC model.

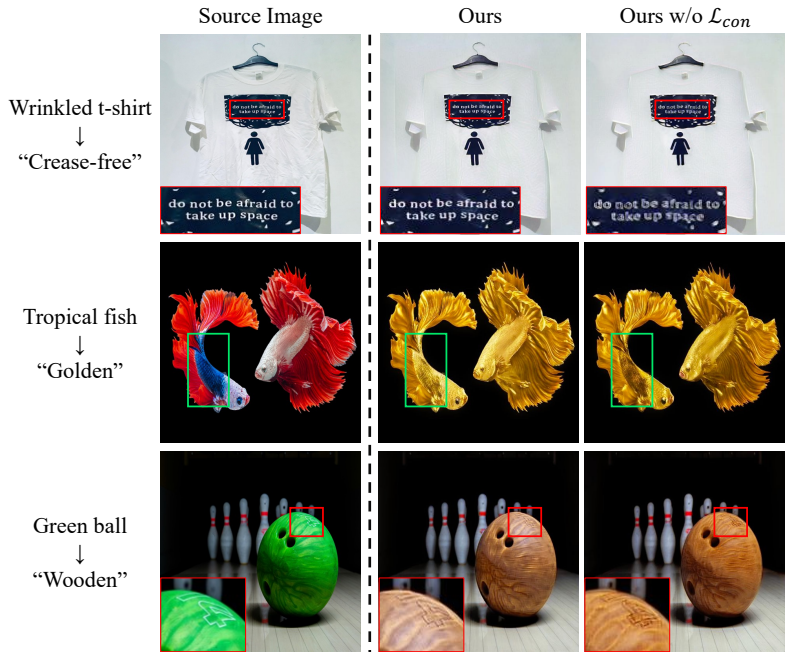


Figure 8. Qualitative comparison demonstrating the effect of the PCD loss by contrasting results with and without the  $\mathcal{L}_{con}$  loss.

## B.2. Visualization of style transfer process

Fig. 9 shows the iterative process of style transfer as conducted by our model. Initially, the model prioritizes the preservation of the background, ensuring it remains as close to the original image as possible. This early focus on background fidelity is a crucial step in maintaining the overall integrity and context of the source image. As the training progresses through successive iterations, the model begins to refine its approach. It gradually learns to enhance and accentuate the details within both the object and the background. This progression illustrates the model’s sophisticated capability to strike a balance between maintaining background fidelity and enhancing the object of interest. This iterative learning and adaptation process is a key aspect of our model’s functionality. It demonstrates how the model evolves to effectively manage the complexities of style transfer, ensuring that both the object’s details and the background’s essence are harmoniously preserved and enhanced.

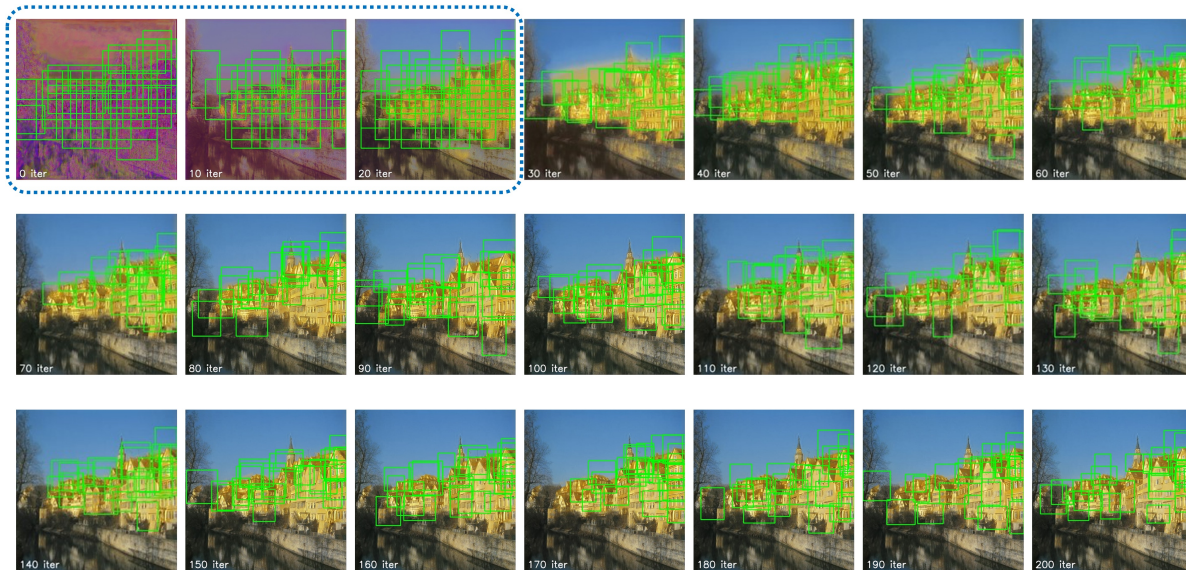


Figure 9. Visualization of the style transfer process at intervals of every 10 iterations. This sequence illustrates the progressive transformation and refinement of the image style over time. The parts marked with blue dashed lines denote the iterations where the Pre-fixed Region Selection module operates, and the green patches in each iteration denote the patches selected through the Text-Matched Patch Selection. Areas not included in the patch are the regions where the Adaptive Background Preservation loss ( $\mathcal{L}_{abp}$ ) is applied.

## B.3. Computational overhead of TMPS and PRS

We conducted additional experiments to assess the computational overhead of the TMPS and PRS modules. In the course of training, we processed the model with 5 distinct styles of text and 3 varieties of source images 10 times to calculate the average time spent. These time estimates encompass both the loading of the CLIP model and the image processing depicted in Tab. 3 -(a), as well as the actual training period shown in Tab. 3 -(b). This data reveals that the proposed modules add merely an extra 10 seconds to the process (see Ours), and that the PRS can indeed reduce training time by approximately 8-9 seconds. This supports our assertion. During the inference phase, which merely involves loading a pre-saved training checkpoint and introducing an image, the presence or absence of any modules does not alter the runtime as shown in Tab. 3 -(c), ensuring consistency across different scenarios. Thus, our experiments illustrate that while the inclusion of the TMPS and PRS modules extends training and inference times, the increase is not significantly detrimental.

Method (seconds)	(a) Total training time (+model & data load)	(b) Training time	(c) Inference time
w/o PRS, w/o TMPS	40.7s	35.2s	0.28s
w/o PRS, w TMPS	59.9s (+19.2s)	53.3s (+18.1s)	0.28s (+0.0s)
w PRS, w TMPS (Ours)	51.9s (+11.2s)	44.3s (+9.1s)	0.28s (+0.0s)

Table 3. Comparison of different methods on training and inference times

### C. Limitations of TEXTOC

A noted limitation of TEXTOC is its reliance on the CLIP model’s feature space and classification capabilities. Consequently, its performance may diminish for styles or objects less represented or absent in the CLIP training dataset, such as recent art or gadgets, as illustrated in Fig. 10. This dependency highlights a potential area for future development, aiming to enhance TEXTOC’s adaptability to emerging styles and objects.

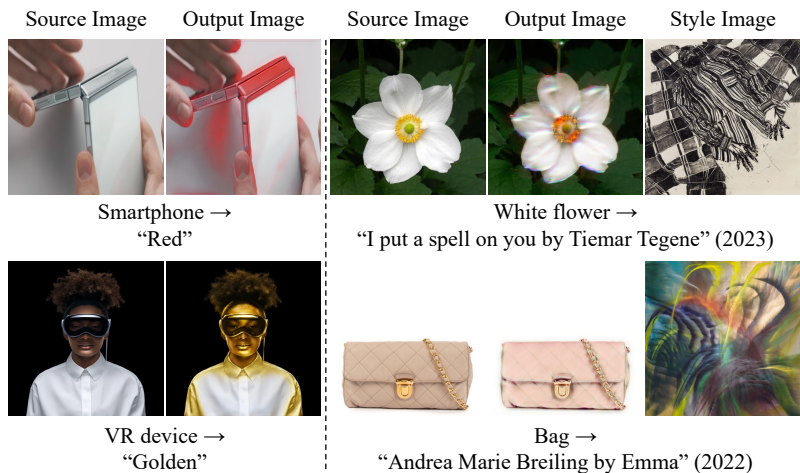


Figure 10. Failure cases of TEXTOC. The numbers following the style text denote the year of the art work was created.

### D. Comparison to mask-guided generative models

In the realm of generative models, significant strides have been made in image generation and editing. Yet, a prevalent challenge among these models, including those guided by masks, is their propensity to inadvertently alter the structural integrity of targeted objects within an image. This often leads to a compromise in the overall image quality and authenticity. To illustrate this limitation and to position our TEXTOC model within the context of current advancements, we conduct a comparative analysis with existing mask-guided generative models [2,38]. These models typically rely on masks to designate specific areas for image editing. Our comparison, as depicted in Fig. 11, highlights a key distinction. Unlike mask-based models, which may inadvertently distort vital details of the object, TEXTOC consistently maintains the structural integrity of the object, focusing solely on altering its style. This distinction is crucial in preserving the overall coherence and authenticity of the image. Moreover, an important advantage of TEXTOC is its autonomous capability to recognize and apply style transfer to objects relevant to the given text. This feature eliminates the cumbersome and often imprecise process of manual mask creation, streamlining the style transfer process. TEXTOC, thus, not only preserves the integrity of the objects but also offers a more efficient and user-friendly approach to style transfer compared to traditional mask-guided generative models.

### E. User study

We conducted the user study to enhance our evaluation process, the results of which are presented in Tab. 4. This study involved 50 participants, whose ages ranged from their 20s to 50s. We designed the study to assess three key aspects: stylization quality, background preservation, and content preservation, providing nine examples within each category for evaluation. We compared the stylized images generated by our model against those produced by Text2live [3], Glide [38], and Blended Diffusion [2], all of which also aim for object-centric style transfer. Our analysis indicates that our model excels in achieving a balanced object-centric style transfer, effectively maintaining the semantic integrity of the object and the background without compromise. The user study question examples illustrated in Fig. 12.

### F. Additional object-centric style transfer results using our TEXTOC

We show additional results of our TEXTOC method, as seen in Fig. 13, Fig. 14, Fig. 15, and Fig. 16. These figures illustrate the effectiveness of our approach in various style transfer scenarios, emphasizing the versatility of TEXTOC. TMPS

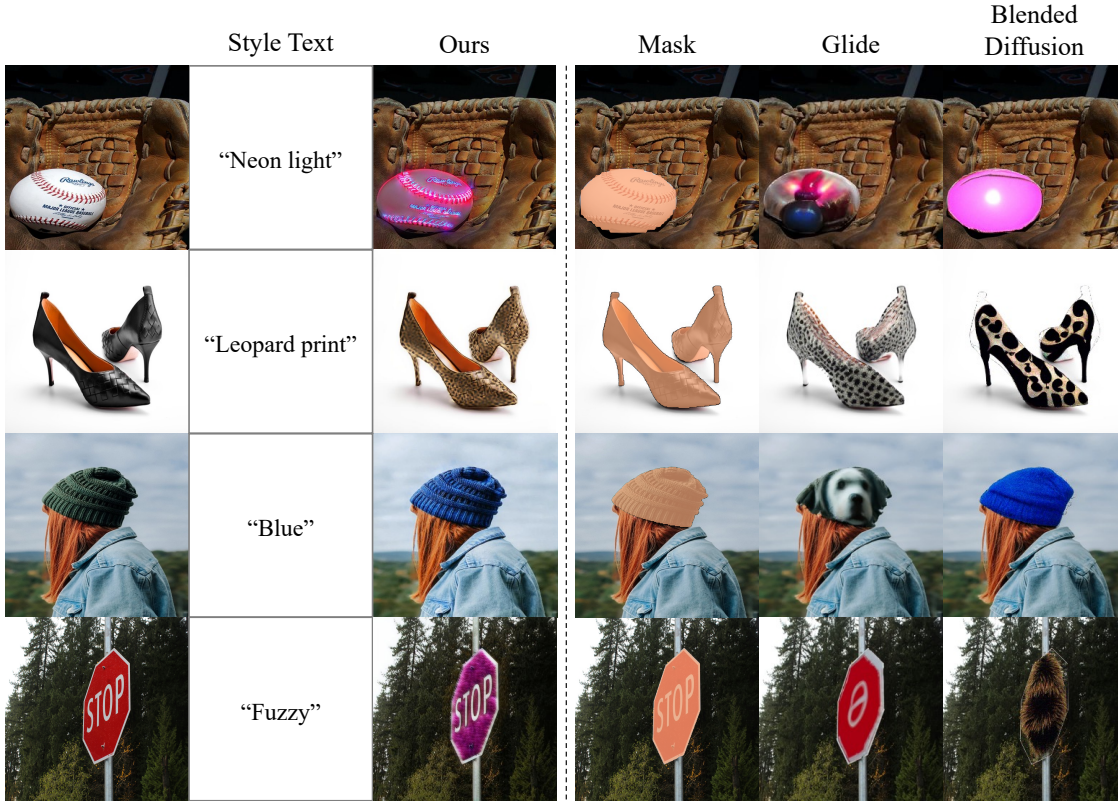


Figure 11. Comparative analysis of TEXTOC with other generative models using mask input. This figure illustrates the effectiveness of our model in handling style transfer challenges where specific object masks are used to guide the process.

Method	StyQual $\uparrow$	BackPre $\uparrow$	ContPre $\uparrow$
Blended Diffusion	4.4 %	7.3 %	2.4 %
Glide	1.1 %	12.0 %	3.6 %
Text2live	29.3%	14.9 %	11.8 %
<b>Ours</b>	<b>65.1 %</b>	<b>65.7 %</b>	<b>82.2 %</b>

Table 4. User study detailing preference percentages.

plays a crucial role in initiating the style transfer process. It specifically targets image areas that correspond with the input text, ensuring that the chosen style is applied seamlessly and appropriately to the relevant objects. This targeted approach results in a harmonious blend of the new style with the original image, particularly in areas corresponding to the source text. Furthermore, our method incorporates an innovative ABP loss. This component of TEXTOC is vital in maintaining the integrity of the background areas during the style transfer process. It ensures that these areas remain unaffected by the changes applied to the object of interest. This loss function is key to achieving a balanced and natural-looking result where the style changes are confined to the targeted object, while the rest of the image retains its original appearance. The results in Fig. 13, Fig. 14, Fig. 15, and Fig. 16 collectively showcase the robust customizability and adaptability of the TEXTOC method. They demonstrate its capability to handle a diverse range of styles and scenarios, effectively adapting the chosen style to the specific objects in the image as dictated by the source text, all while preserving the overall aesthetic and integrity of the background.

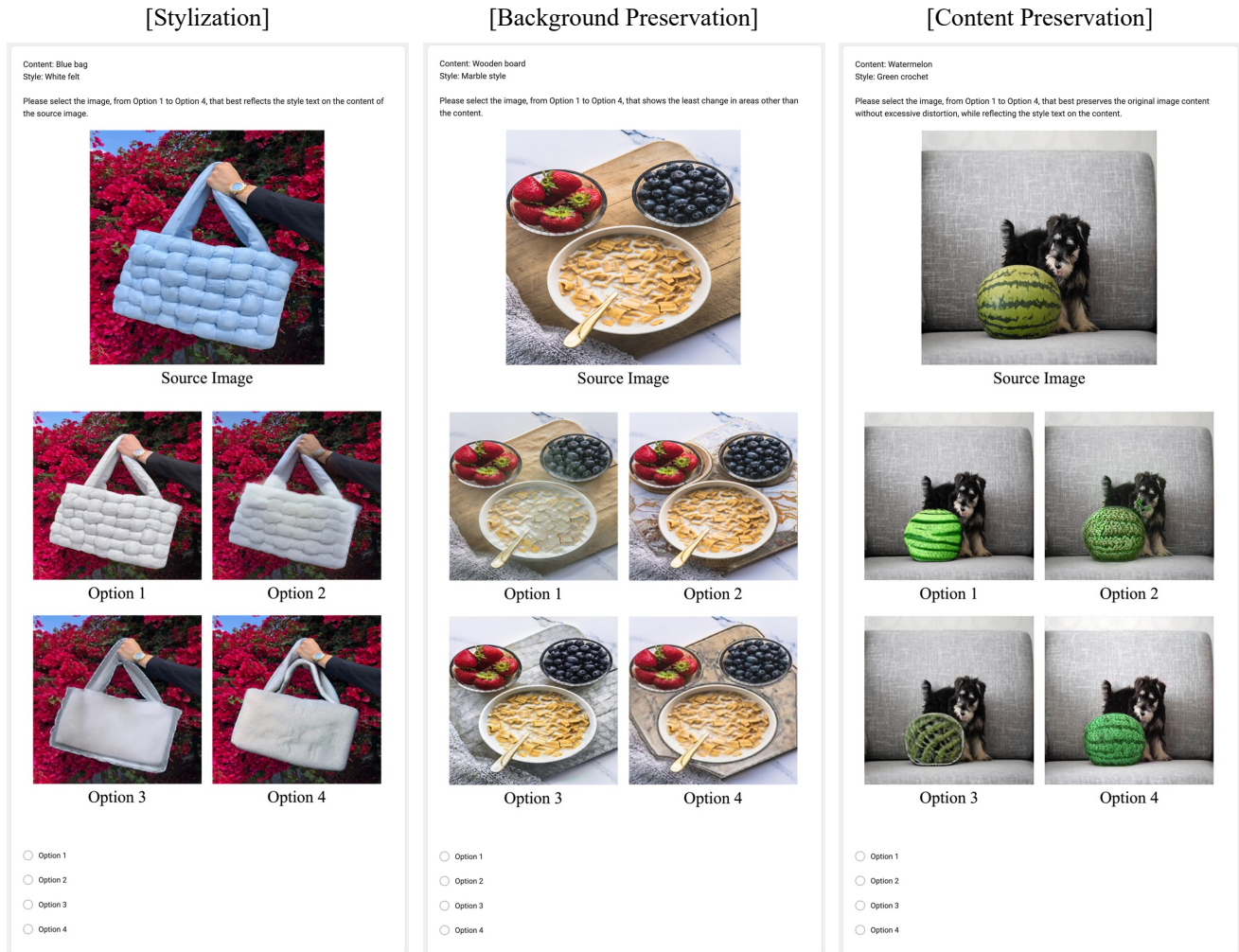


Figure 12. User study question examples. The order of options was shuffled for each question.



Figure 13. Stylization results demonstrating various "artistic" styles guided by text using our TEXTOC model.



Figure 14. Stylization results demonstrating various “color” styles guided by text using our TEXTOC model.



Figure 15. Stylization results demonstrating various “texture” styles guided by text using our TEXTOC model.



Figure 16. Our additional stylization results with various image-text scenarios.

## References

- [1] Jie An, Siyu Huang, Yibing Song, Dejing Dou, Wei Liu, and Jiebo Luo. Artflow: Unbiased image style transfer via reversible neural flows, 2021. [2](#)
- [2] Omri Avrahami, Dani Lischinski, and Ohad Fried. Blended diffusion for text-driven editing of natural images. In *Proceedings of the IEEE/CVF Conference on Computer Vision and Pattern Recognition*, pages 18208–18218, 2022. [12](#)
- [3] Omer Bar-Tal, Dolev Ofri-Amar, Rafail Fridman, Yoni Kasten, and Tali Dekel. Text2live: Text-driven layered image and video editing, 2022. [2](#), [3](#), [6](#), [12](#)
- [4] Tim Brooks, Aleksander Holynski, and Alexei A Efros. Instructpix2pix: Learning to follow image editing instructions. In *Proceedings of the IEEE/CVF Conference on Computer Vision and Pattern Recognition*, pages 18392–18402, 2023. [2](#), [6](#)
- [5] Hila Chefer, Shir Gur, and Lior Wolf. Generic attention-model explainability for interpreting bi-modal and encoder-decoder transformers, 2021. [3](#)
- [6] Haibo Chen, Zhizhong Wang, Huiming Zhang, Zhiwen Zuo, Ailin Li, Wei Xing, Dongming Lu, et al. Artistic style transfer with internal-external learning and contrastive learning. *Advances in Neural Information Processing Systems*, 34:26561–26573, 2021. [2](#)
- [7] Guillaume Couairon, Asya Grechka, Jakob Verbeek, Holger Schwenk, and Matthieu Cord. Flexit: Towards flexible semantic image translation, 2022. [6](#)
- [8] Katherine Crowson, Stella Biderman, Daniel Kornis, Dashiell Stander, Eric Hallahan, Louis Castricato, and Edward Raff. Vqgan-clip: Open domain image generation and editing with natural language guidance, 2022. [2](#)
- [9] Jacob Devlin, Ming-Wei Chang, Kenton Lee, and Kristina Toutanova. Bert: Pre-training of deep bidirectional transformers for language understanding, 2019. [4](#)
- [10] Keyan Ding, Kede Ma, Shiqi Wang, and Eero P. Simoncelli. Image quality assessment: Unifying structure and texture similarity. *IEEE Transactions on Pattern Analysis and Machine Intelligence*, pages 1–1, 2020. [5](#)
- [11] Alexey Dosovitskiy, Lucas Beyer, Alexander Kolesnikov, Dirk Weissenborn, Xiaohua Zhai, Thomas Unterthiner, Mostafa Dehghani, Matthias Minderer, Georg Heigold, Sylvain Gelly, et al. An image is worth 16x16 words: Transformers for image recognition at scale. *arXiv preprint arXiv:2010.11929*, 2020. [5](#)
- [12] Vincent Dumoulin, Jonathon Shlens, and Manjunath Kudlur. A learned representation for artistic style. *arXiv preprint arXiv:1610.07629*, 2016. [2](#)
- [13] Fernando A. Fardo, Victor H. Conforto, Francisco C. de Oliveira, and Paulo S. Rodrigues. A formal evaluation of psnr as quality measurement parameter for image segmentation algorithms, 2016. [5](#)
- [14] Kevin Frans, L. B. Soros, and Olaf Witkowski. Clipdraw: Exploring text-to-drawing synthesis through language-image encoders, 2021. [2](#)
- [15] Tsu-Jui Fu, Xin Eric Wang, and William Yang Wang. Language-driven image style transfer, 2022. [2](#)
- [16] Rinon Gal, Or Patashnik, Haggai Maron, Gal Chechik, and Daniel Cohen-Or. Stylegan-nada: Clip-guided domain adaptation of image generators, 2021. [2](#), [4](#)
- [17] Leon A. Gatys, Alexander S. Ecker, and Matthias Bethge. Image style transfer using convolutional neural networks. In *Proceedings of the IEEE Conference on Computer Vision and Pattern Recognition (CVPR)*, June 2016. [2](#), [3](#), [5](#)
- [18] Jiayi Guo, Chaofei Wang, You Wu, Eric Zhang, Kai Wang, Xingqian Xu, Shiji Song, Humphrey Shi, and Gao Huang. Zero-shot generative model adaptation via image-specific prompt learning, 2023. [2](#)
- [19] Jonathan Ho, Ajay Jain, and Pieter Abbeel. Denoising diffusion probabilistic models, 2020. [2](#)
- [20] Matthew Honnibal and Mark Johnson. An improved non-monotonic transition system for dependency parsing. In Lluís Màrquez, Chris Callison-Burch, and Jian Su, editors, *Proceedings of the 2015 Conference on Empirical Methods in Natural Language Processing*, pages 1373–1378, Lisbon, Portugal, Sept. 2015. Association for Computational Linguistics. [4](#)
- [21] Xun Huang and Serge Belongie. Arbitrary style transfer in real-time with adaptive instance normalization. In *Proceedings of the IEEE International Conference on Computer Vision (ICCV)*, Oct 2017. [2](#)
- [22] Xun Huang and Serge Belongie. Arbitrary style transfer in real-time with adaptive instance normalization, 2017. [5](#)
- [23] Zixuan Huang, Jinghui Zhang, and Jing Liao. Style mixer: Semantic-aware multi-style transfer network. In *Computer Graphics Forum*, volume 38, pages 469–480. Wiley Online Library, 2019. [2](#)
- [24] Jing Huo, Shiyin Jin, Wenbin Li, Jing Wu, Yu-Kun Lai, Yinghuan Shi, and Yang Gao. Manifold alignment for semantically aligned style transfer, 2021. [2](#)
- [25] Sargan Jandial, Shripad Deshmukh, Abhinav Java, Simra Shahid, and Balaji Krishnamurthy. Gatha: Relational loss for enhancing text-based style transfer. In *Proceedings of the IEEE/CVF Conference on Computer Vision and Pattern Recognition*, pages 3545–3550, 2023. [2](#)
- [26] Justin Johnson, Alexandre Alahi, and Li Fei-Fei. Perceptual losses for real-time style transfer and super-resolution, 2016. [2](#), [5](#)
- [27] Chanda G Kamra, Indra Deep Mastan, and Debayan Gupta. Sem-cs: Semantic clipstyler for text-based image style transfer. 2023. [2](#), [3](#)
- [28] Tero Karras, Samuli Laine, and Timo Aila. A style-based generator architecture for generative adversarial networks. In *Proceedings of the IEEE/CVF conference on computer vision and pattern recognition*, pages 4401–4410, 2019. [2](#)
- [29] Tero Karras, Samuli Laine, Miika Aittala, Janne Hellsten, Jaakko Lehtinen, and Timo Aila. Analyzing and improving the image quality of stylegan, 2020. [2](#)
- [30] Diederik P Kingma and Jimmy Ba. Adam: A method for stochastic optimization. *arXiv preprint arXiv:1412.6980*, 2014. [5](#)
- [31] Lironne Kurzman, David Vazquez, and Issam Laradji. Class-based styling: Real-time localized style transfer with semantic segmentation, 2019. [2](#)

- [32] Gihyun Kwon and Jong Chul Ye. Clipstyler: Image style transfer with a single text condition. In *Proceedings of the IEEE/CVF Conference on Computer Vision and Pattern Recognition*, pages 18062–18071, 2022. 2, 3, 4, 6
- [33] Yijun Li, Chen Fang, Jimei Yang, Zhaowen Wang, Xin Lu, and Ming-Hsuan Yang. Diversified texture synthesis with feed-forward networks. In *Proceedings of the IEEE conference on computer vision and pattern recognition*, pages 3920–3928, 2017. 2
- [34] Yijun Li, Chen Fang, Jimei Yang, Zhaowen Wang, Xin Lu, and Ming-Hsuan Yang. Universal style transfer via feature transforms, 2017. 2
- [35] Yijun Li, Ming-Yu Liu, Xueting Li, Ming-Hsuan Yang, and Jan Kautz. A closed-form solution to photorealistic image stylization, 2018. 2
- [36] Tsung-Yi Lin, Michael Maire, Serge Belongie, Lubomir Bourdev, Ross Girshick, James Hays, Pietro Perona, Deva Ramanan, C. Lawrence Zitnick, and Piotr Dollár. Microsoft coco: Common objects in context, 2015. 6
- [37] Ron Mokady, Amir Hertz, Kfir Aberman, Yael Pritch, and Daniel Cohen-Or. Null-text inversion for editing real images using guided diffusion models. In *Proceedings of the IEEE/CVF Conference on Computer Vision and Pattern Recognition*, pages 6038–6047, 2023. 6
- [38] Alex Nichol, Prafulla Dhariwal, Aditya Ramesh, Pranav Shyam, Pamela Mishkin, Bob McGrew, Ilya Sutskever, and Mark Chen. Glide: Towards photorealistic image generation and editing with text-guided diffusion models, 2022. 2, 12
- [39] Adam Paszke, Sam Gross, Francisco Massa, Adam Lerer, James Bradbury, Gregory Chanan, Trevor Killeen, Zeming Lin, Natalia Gimelshein, Luca Antiga, et al. Pytorch: An imperative style, high-performance deep learning library. *Advances in neural information processing systems*, 32, 2019. 5
- [40] Or Patashnik, Zongze Wu, Eli Shechtman, Daniel Cohen-Or, and Dani Lischinski. Styleclip: Text-driven manipulation of stylegan imagery. In *Proceedings of the IEEE/CVF International Conference on Computer Vision*, pages 2085–2094, 2021. 2
- [41] Justin N. M. Pinkney and Chuan Li. clip2latent: Text driven sampling of a pre-trained stylegan using denoising diffusion and clip, 2022. 2
- [42] Alec Radford, Jong Wook Kim, Chris Hallacy, Aditya Ramesh, Gabriel Goh, Sandhini Agarwal, Girish Sastry, Amanda Askell, Pamela Mishkin, Jack Clark, et al. Learning transferable visual models from natural language supervision. In *International conference on machine learning*, pages 8748–8763. PMLR, 2021. 2
- [43] Alec Radford, Karthik Narasimhan, Tim Salimans, and Ilya Sutskever. Improving language understanding by generative pre-training. 2018. 4
- [44] Olaf Ronneberger, Philipp Fischer, and Thomas Brox. U-net: Convolutional networks for biomedical image segmentation. In *Medical Image Computing and Computer-Assisted Intervention—MICCAI 2015: 18th International Conference, Munich, Germany, October 5-9, 2015, Proceedings, Part III 18*, pages 234–241. Springer, 2015. 5
- [45] Leonid I Rudin, Stanley Osher, and Emad Fatemi. Nonlinear total variation based noise removal algorithms. *Physica D: nonlinear phenomena*, 60(1-4):259–268, 1992. 3
- [46] Nataniel Ruiz, Yuanzhen Li, Varun Jampani, Yael Pritch, Michael Rubinstein, and Kfir Aberman. Dreambooth: Fine tuning text-to-image diffusion models for subject-driven generation, 2023. 2
- [47] Chitwan Saharia, William Chan, Saurabh Saxena, Lala Li, Jay Whang, Emily Denton, Seyed Kamyar Seyed Ghasemipour, Burcu Karagol Ayan, S. Sara Mahdavi, Rapha Gontijo Lopes, Tim Salimans, Jonathan Ho, David J Fleet, and Mohammad Norouzi. Photorealistic text-to-image diffusion models with deep language understanding, 2022. 2
- [48] Peter Schaldenbrand, Zhixuan Liu, and Jean Oh. Styleclip-draw: Coupling content and style in text-to-drawing translation, 2022. 2
- [49] Narek Tumanyan, Michal Geyer, Shai Bagon, and Tali Dekel. Plug-and-play diffusion features for text-driven image-to-image translation, 2022. 6
- [50] Dmitry Ulyanov, Vadim Lebedev, Andrea Vedaldi, and Victor Lempitsky. Texture networks: Feed-forward synthesis of textures and stylized images. *arXiv preprint arXiv:1603.03417*, 2016. 2
- [51] Dmitry Ulyanov, Andrea Vedaldi, and Victor Lempitsky. Instance normalization: The missing ingredient for fast stylization. *arXiv preprint arXiv:1607.08022*, 2016. 2
- [52] Zhou Wang, A.C. Bovik, H.R. Sheikh, and E.P. Simoncelli. Image quality assessment: from error visibility to structural similarity. *IEEE Transactions on Image Processing*, 13(4):600–612, 2004. 5
- [53] Serin Yang, Hyunmin Hwang, and Jong Chul Ye. Zero-shot contrastive loss for text-guided diffusion image style transfer, 2023. 2, 6
- [54] Zhenling Yang, Huacheng Song, and Qiunan Wu. Generative artisan: A semantic-aware and controllable clipstyler, 2022. 3
- [55] Moon Ye-Bin, Jisoo Kim, Hongyeob Kim, Kilho Son, and Tae-Hyun Oh. Textmania: Enriching visual feature by text-driven manifold augmentation, 2023. 4
- [56] Yingchen Yu, Fangneng Zhan, Rongliang Wu, Jiahui Zhang, Shijian Lu, Miaomiao Cui, Xuansong Xie, Xian-Sheng Hua, and Chunyan Miao. Towards counterfactual image manipulation via clip. In *Proceedings of the 30th ACM International Conference on Multimedia*, pages 3637–3645, 2022. 2